Energy Transfer in MHD Convective Heat and Specie Flow of Cu – H_2O Nanofluid in a Porous Channel with Stationary Walls

Amadi, Okechukwu[1], Amos, Emeka[2]

[1]*Department of Mathematics/Statistics, Ignatius Ajuru University of Education, P.M.B 5047 Rumuolumeni, Nigeria*
[2]*Department of Mathematics/Statistics, Rivers State University, P.M.B 5080 Nkpolu-Oroworukwo, Nigeria*

Abstract: **The study investigated thermal transfer in magnetohydrodynamics(MHD) convective flow of Cu-H_2O nanofluid in a porous medium with heat generation/absorption. A set of partial differential equations with copper nanoparticles were used. The partial differential equations were non-dimensioned with various dimensionless quantities in order to obtain forms whose solutions can be easily obtained. The partial differential equations were later transformed into ordination differential equations through a two term perturbation technique which were later solved using method of undetermined coefficient to obtain the exact solutions for the energy, concentration and momentum equations. Using the exact solutions; plots were done with the aid of standard parameters to estimate the variational effects of parameters that entered the flow field. From the plots; it was observed that thermal radiation decreased the temperature of the fluid. Heat generation/absorption parameter increased the temperature of the fluid. The effective thermal conductivity increased the temperature of the fluid. Peclet number and Reynolds number decreased the fluid velocity, increasing the Schmidt number and frequency of oscillation increased the concentration of the fluid.**

Keywords: **Heat transfer, Porous medium, Heat generation, Nanofluid, Magnetohydrodynamics(MHD)**

I. INTRODUCTION

Thermal conductivity plays a vital role in warmness transfer enhancement. Conventional heat switch fluids along with water, ethylene glycol (EG), kerosene oil and lubricant oils have negative thermal conductivities compared to solids. Solids debris however has better thermal conductivities in comparison to traditional warmth switch fluids. Choi (1995) in his pioneering paintings indicated that when a small quantity of nanoparticles is added to not unusual base fluids, it will increase extensively the thermal conductivity of the base fluids in addition to their convective warmness transfer rate. This combination is known as nanofluids. More precisely, nanofluids are suspensions of nano-length debris in base fluids. Usually nanofluids include specific sorts of nanoparticles inclusive of oxides, metals and carbides in generally base fluids like water, EG, propylene glycol and kerosene oil. Some unique packages of nanofluids are located in various digital equipment, energy supply, energy generation, air con and manufacturing. Vajjha and Das (2009) for the first time used EG (60 %) and water (40 %) aggregate as base fluid for the preparation of alumina (Al_2O_3), copper oxide (CuO) and zinc oxide (ZnO) nanofluids. At the identical temperature and attention, they observed that CuO nanofluid posses excessive thermal conductivity evaluate to the ones of Al_2O_3 and ZnO nanofluids. Naik and Sundar (2011) took 70 % propylene glycol and 30 % water and prepared CuO nanofluid. As expected, they found that CuO nanofluid has better thermal conductivity and viscosity homes compare to base fluid. Malvandi et al.(2013) studied entropy generation of nanofluids over a plate analytically. They used the homotopy-pertubation method (HPM) and the variational iteration method (VIM) to solve the nonlinear ordinary differential equation. It was noted that the high density of Cu added as nanoparticles to water generates more entropy in contrast to other nanoparticles in a process. Murugesan and Kumar.(2019) embarked on the study viscous dissipation and joule heating effects on thermo solutal stratified nanofluid over a stretching sheet. They remarked that Schmidt number decreases the temperature after obtaining a numerical solution of the nonlinear ordinary differential equations. Khan et al.(2012) studied the unsteady mhd free convection of nanofluid along a stretching sheet with thermal radiation. They obtained different time steps and for the different values of the parameters of physical and engineering interest. Natural convection flow of fractional nanofluids over an isothermal vertical plate with thermal radiation was studied by Constantin et al.(2017). The fluid temperature increases for increasing values of the nanoparticle volume fraction was noted by them after obtaining the closed form solution and plotting the graph. Latiff et al.(2016) studied Stefan blowing effect of nanofluid over a solid rotating stretchable disk. The nonlinear ordinary differential equations were solved numerically using the Runge-Kutta-Fehlberg method. It was remarked that the Stefan blowing increases the local skin friction and reduces the heat transfer, mass transfer and microorganism transfer rates. Second order slip flow of Cu-Water nanofluid over a stretching sheet with heat transfer was undergone by Rajesh et al.(2014). They solved the differential equations using finite element method. They showed the

effects of parameters variation with the aid of graphs. Aaiza et al.(2015) studied energy transfer in nanofluid containing different shapes of nanoparticles. They found that viscosity and thermal conductivity are the most prominent parameters responsible for different results of velocity and temperature.

The concept of heat generating and absorbing fluid cannot be ignored due to its significance in problems dealing with chemical reactions. Heat generation effects may alter the temperature distribution and this in turn can impact the particle deposition rate in nuclear reactors, electronic chips and semi conductor wafers. Though the exact modeling of internal heat generation or absorption in its sense is difficult to combat but some simple mathematical models can be used to express its general behavior for most of the physical circumstances. It is assumed to be constant, space-dependent or temperature –dependent. A host of authors have dealt with this concept. Murugesan and Kumar. (2019) studied viscous dissipation of nanofluid over a stretching sheet with heat generation. They solved the nonlinear models adopting a numerical approach of Nachitsheim-Swigert shooting technique scheme together with Runge Kutta fourth order. Remarkably they noted that heat generation increased the temperature of the fluid under consideration. Mass transfer and heat generation effects was embarked on by Reddy and Reddy(2011). They considered the mhd free convection in connection to it. They adopted the Runge Kutta fourth order with shooting technique to solve the problems. They noted that heat generation increased both the velocity and temperature of the fluid.

Studies have shown that energy transfer via a porous medium has obtained investigations from enormous researchers significantly because of its usage in contemporary technologies. The porous medium has the tenacity to change the flow field and influence the rate of heat being transfer. In view of the foregoing Madhura et al.(2017) investigated the impact of heat and mass transfer on mixed convection. They adopted laplace transformation to obtain the closed form solution and noted in the result that porosity abet the velocity of the flow when increased. Madhura et al.(2020) studied heat mass transfer of MHD fluid flow under the influence of radiative effect and different pressure gradients. The finite difference method was adopted. The result obtained showed that permeability increased the rate of heat transfer. Kathyayani et al.(2016) examined heat and mass transfer on MHD flow over an infinite rotating oscillating vertical porous plate. Outstandingly, they noted that porosity influenced the rate of fluid flow.

Magnetohydrodynamics (MHD) is the science which is associated with the motion of exceedingly conducting liquids in the presence of a magnetic field. The motion of the conducting liquid throughout the magnetic area generates electric currents which change the magnetic field, and the motion of the magnetic field on those currents offers upward thrust to mechanical forces which alter the drift of the liquid. MHD combines both standards of fluid dynamics and electromagnetism. MHD considers the magnetic properties of electrically conducting fluids. When an electrically conducting fluid moves through a magnetic field, an electric field may be brought on and will interact with the magnetic properties to supply a body pressure. The science which deals with this phenomenon is referred to as magnetohydrodynamics. Owing to the significance of this concept; so many authors halve delved into it. Soret effect on MHD free convection through a porous inclined channel was embarked upon by Achogo et al.(2020). They noted that soret number increases both the concentration and velocity profiles after obtaining the closed form analytically through the method of undetermined coefficient. Reddy et al.(2011) examined mass transfer and heat generation effects on MHD free convection flow past an inclined vertical surface ina porous medium. They solved the nonlinear systems through a numerical approach by applying the Runge-Kutta method of fourth order with shooting technique. Buggaramulu and Venta.(2017) studied MHD convection flow of Kuvshinski fluid past an infinite vertical porus plate. The nonlinear equations were solved by adopting a two term perturbation technique and they solved analytically. Shatey et. Al(2015) studied on spectral relaxation method for entropy generation on mhd flow and heat transfer of a Maxwell fluid. Srinivasacharya and Bindu(2015) examined entropy generation in a mhd micro polar fluid flow through an inclined channel.

In this paper, we considered energy transfer in mhd convective heat and specie flow of cu – h_2o nanofluid in a porous channel with stationary walls.

II. FORMULATION OF THE PROBLEM

The following assumptions were made;

a) The flow is oscillatory of nanofluids.
b) The fluid is electrically conducting in the presence of uniform magnetic field applied perpendicularly to the direction of flow.
c) The magnetic Reynolds number is very small such that the impact of induced magnetic field is forfeited.
d) The external electric field is considered zero and the electric field due to polarization is negligible.
e) The no-slip condition at the boundary walls is considered.
f) The x-axis is taken along the flow and y-axis is taken normal to the direction of flow.
g) The natural convection results from buoyancy force together with external pressure gradient applied along the x-direction.
h) T_0 and T_w are considered very high enough to induce the radiative heat transfer.

i) C_0 and C_w are considered very high enough to induce mass transfer.

j) Going by the Boussinesq approximation, the governing equations of momentum and energy are as follows;

$$\rho_{nf}\left(\frac{\partial u'}{\partial t'}+v'\frac{\partial u'}{\partial y'}\right)=-\frac{\partial p'}{\partial x'}+\mu_{nf}\frac{\partial^2 u'}{\partial y'^2}-\frac{\mu_{nf}}{K}u'-\sigma\beta_0^2u'+g(\rho\beta)_{nf}(T'-T_0)+g(\rho\beta)_{nf}(C'-C_0) \quad (1)$$

$$\left(\rho c_p\right)_{nf}\left(\frac{\partial T'}{\partial t'}+v'\frac{\partial T'}{\partial y'}\right)=k_{nf}\frac{\partial^2 T'}{\partial y'^2}-\frac{\partial q_r'}{\partial y'}-Q_0(T'-T_0) \quad (2)$$

$$\left(\rho c_p\right)_{nf}\left(\frac{\partial C'}{\partial t'}+v'\frac{\partial C'}{\partial y'}\right)=D_{nf}\frac{\partial^2 C'}{\partial y'^2}-Kr'(C'-C_0) \quad (3)$$

Where u=u(y,t) represents the velocity in the direction of x, T=T(y,t) the temperature, C=C(y,t) the concentration, ρ_{nf} the density, μ_{nf} the dynamic viscosity of the nanofluid, σ the electrical conductivity of the base fluid, K> 0 the permeability of the porous medium, $(\rho\beta)_{nf}$ thermal expansion coefficient of nanofluid, g the acceleration due to gravity, $\left(\rho c_p\right)_{nf}$ the heat capacitance of nanofluids, k_{nf} the thermal conductivity of nanofluid, q_r the radiative heat flux in x-direction, p the external pressure, Q_0 the heat generation/absorption, Kr the chemical reaction term

The boundary condition expedient are as follows;

$y'=0$; $u'=0$, $T'=T_0$, $C'=C_0$ (4a)

$y'=d$; $u'=0$, $T'=T_w$, $C'=C_w$ (4b)

Following the Hamilton and Crosser model(1962),the dynamic viscosity of the nanofluid(μ_{nf}), thermal expansion coefficient of nanofluid($(\rho\beta)_{nf}$), heat capacitance of nanofluids($\left(\rho c_p\right)_{nf}$), thermal conductivity of nanofluid(k_{nf}) are;

$$\mu_{nf}=\mu_f(1+a\emptyset+b\emptyset^2) \quad (5a)$$

$$\frac{k_{nf}}{k_f}=\frac{k_s+(n-1)k_f+(n-1)(k_s-k_f)\emptyset}{k_s+(n-1)k_f+(k_s-k_f)\emptyset} \quad (5b)$$

$$\rho_{nf}=(1-\emptyset)\rho_f+\emptyset\rho_s \quad (5c)$$

$$(\rho\beta)_{nf}=(1-\emptyset)(\rho\beta)_f+\emptyset(\rho\beta)_s \quad (5d)$$

$$\left(\rho c_p\right)_{nf}=(1-\emptyset)\left(\rho c_p\right)_f+\emptyset\left(\rho c_p\right)_s \quad (5e)$$

$\emptyset$ denotes the nanoparticles volume fraction, ρ_f and ρ_s are the densities of the base fluid and solid nanoparticles, β_s and β_f are the volumetric expansion coefficients of thermal expansions of solid nanopartiles and base fluids,$\left(c_p\right)_s$ and $\left(c_p\right)_f$ are the specific heat capacities of solid nanoparticles and base fluids at constant pressure, a and b represent constants and find their values on the particle shape as represented by Aaiza et al.(2015) in Table 1. The n in equation (4b) denotes the empirical shape factor and it is expressed as $n=\frac{3}{\Psi}$, where Ψ means the sphericity which denotes the ratio between the surface are of the sphere and the surface area of the real particle with equal volumes(Aiza et al.(2015)). The Ψ is clearly seen in Table 2.

Table1: Constants a and b empirical shape factors

Model	Platelet	Blade	Cylinder	Brick
A	37.1	14.6	13.5	1.9
B	612.6	123.3	904.4	471.4

Table 2: Sphericity Ψ for different shapes nanoparticles

Model	Platelet	Blade	Cylinder	Brick
Ψ	0.52	0.36	0.62	0.81

Table 3: Thermophysical properties of water and nanoparticles

Model	$\rho(kgm^{-3})$	$c_p(kg^{-1}K^{-1})$	$k(Wm^{-1}K^{-1})$	$\beta \times 10^{-5}(K^{-1})$
Pure water(H_2O)	997.1	4179	0.613	21
Copper(Cu)	8933	385.0	401.0	1.67

Following Cogley et al.(1968) for optically thin fluid with relatively low density, the heat flux is expressed as;

$$\frac{\partial q_r}{\partial y}=-4\alpha^2(T'-T_0) \quad (6)$$

The symbol α denotes the mean radiation absorption coefficient.

Now introducing equation (5) into equation (2), it yields;

$$\left(\rho c_p\right)_{nf}\left(\frac{\partial T'}{\partial t'}+v'\frac{\partial T'}{\partial y'}\right)=k_{nf}\frac{\partial^2 T'}{\partial y'^2}+4\alpha^2(T'-T_0)-Q_0(T'-T_0) \quad (7)$$

Now we introduce the following dimensionless quantities into equations (1) and (6)

$$x = \frac{x'}{d}, y = \frac{y'}{d}, u = \frac{u'}{U_0}, t = \frac{tU_0}{d}, p = \frac{d}{\mu U_0}p', T = \frac{T' - T_0}{T_w - T_0}, C = \frac{C' - C_0}{C_w - C_0}, , \omega = \frac{d\omega'}{U_0}, \varepsilon = \frac{\mu}{\mu_f},$$

$$\frac{\partial p}{\partial x} = \lambda e^{i\omega t}, \quad Re = \frac{U_0 d}{v_f}, M^2 = \frac{\sigma B_0^2 d^2}{\mu_f}, K = \frac{K'}{d^2}, Gr = \frac{g\beta_f d^2(T_w - T_0)}{v_f U_0}, Pe_t = \frac{U_0 d(\rho c_p)_f}{k_f}, N^2 = \frac{4d^2\alpha^2}{k_f},$$

$$\lambda n = \frac{k_{nf}}{k_f}, S = \frac{Q_0 d^2}{k_f}, \eta = \frac{1}{U_0}, v = \frac{v'}{v_0}, Pe_c = \frac{U_0 d(\rho c_p)_f}{D_{nf}}, Gr = \frac{g\beta_f d^2(C_w - C_0)}{v_f U_0}, Sc = \frac{v}{D_{nf}}, Kr = \frac{Kr' d}{v}$$

Together with equations (4a)-(4e) appropriately.

Re is the Reynolds number, M is the magnetic parameter also known as the Hartmann number, K is the permeability, Gr is the thermal Grashof number, Gm is the solutal Grashof number, Pe is the Peclet number owing to temperature and concentration respectively, N is the radiation parameter, S is the heat generation parameter, Sc the Schmidt number, Kr chemical reaction parameter.

A close look at the continuity equation shows that the suction velocity normal to the channel is a function of time and shall therefore be taken as;

$$v' = v_0(1 + \epsilon A e^{nt}) \quad (8)$$

The following were obtained;

$$m_4 Re\left(\frac{\partial u}{\partial t} - m_2\frac{\partial u}{\partial y}\right) = \lambda e^{i\omega t} + m_5\frac{\partial^2 u}{\partial y^2} + \left(M^2 + \frac{m_5}{K}\right)u + m_6 GrT + m_6 GmC \quad (9)$$

$$\frac{m_1 Pe_t}{\lambda n}\left(\frac{\partial T}{\partial t} - m_2\frac{\partial T}{\partial y}\right) = \frac{\partial^2 T}{\partial y^2} + \frac{N^2 - S}{\lambda n}T \quad (10)$$

$$m_1 Pe_c\left(\frac{\partial C}{\partial t} - m_2\frac{\partial C}{\partial y}\right) = \frac{\partial^2 C}{\partial y^2} + KrScC \quad (11)$$

where $m_1 = 1 - \phi + \phi\frac{(\rho c_p)_s}{(\rho c_p)_f}, m_2 = \eta(1 + \epsilon A e^{nt}), m_5 = 1 + a\emptyset + b\emptyset^2, m_4 = 1 - \phi + \phi\frac{\rho_s}{\rho_f},$

$$m_6 = 1 - \phi + \phi\frac{(\rho\beta)_s}{(\rho\beta)_f}$$

with the boundary conditions as;

y=0; u=0, T=0, C=0 (12a)

y=1; u=0, T=1, C=1 (12b)

We now assume pertubation solutions for the momentum and temperature of the forms below;

$u(y,t)=u_0(y)+u_1(y)\epsilon e^{i\omega t}$ (13)

$T(y,t)=T_0(y)+T_1(y)\,\epsilon e^{i\omega t}$ (14)

$C(y,t)= C_0(y)+C_1(y)\,\epsilon e^{i\omega t}$ (15)

Adopting equations (11) - (13) in equations (8) - (10), we obtain ordinary differential equations depending on the space coordinate only as follows;

$$m_5\frac{d^2u_0}{dy^2} + m_2 m_4 Re\frac{du_0}{dy} - \left(M^2 + \frac{m_5}{K}\right)u_0 = -m_6 Gr\theta_0 \quad (16)$$

$$m_5\frac{d^2u_1}{dy^2} + m_2 m_4 Re\frac{du_1}{dy} - \left(M^2 + \frac{m_5}{K} + m_4 Rei\omega\right)u_1 = -\lambda - m_6 Gr\theta_1 \quad (17)$$

$$\frac{d^2T_0}{dy^2} + \frac{m_2 m_1 Pe}{\lambda n}\frac{dT_0}{dy} + \frac{(N^2 - S)}{\lambda n}T_0 = 0 \quad (18)$$

$$\frac{d^2T_1}{dy^2} + \frac{m_2 m_1 Pe}{\lambda n}\frac{dT_1}{dy} + \frac{(-N^2 + S + m_1 Pei\omega)}{\lambda n}T_1 = 0 \quad (19)$$

$$\frac{d^2C_0}{dy^2} + m_2 m_1 Pe_c\frac{dC_0}{dy} - KrScC_0 = 0 \quad (20)$$

$$\frac{d^2C_1}{dy^2} + m_2 m_1 Pe_c\frac{dC_1}{dy} - (m_1 Pe_c i\omega + KrScC_1) = 0 \quad (21)$$

The boundary conditions also as;

y=0; u_0=0,u_1=0, $T_0 = 0, T_1 = 0, C_0 = 0, C_1 = 0$ (22a)

y=1; u_0=0,u_1=0, $T_0 = 1, T_1 = 0, C_0 = 1 \quad , C_1 = 0$ (22b)

We proceeded to solve equations (14)-(19) together with the appropriate boundary conditions (equation 20a and 20b) and obtained;

$u_0(y)=D_5 e^{\alpha_5 y} + D_6 e^{\alpha_6 y} + D_7 e^{\alpha_1 y} + D_8 e^{\alpha_2 y} + D_9 e^{\alpha_3 y} + D_{10} e^{\alpha_4 y}$ (23)

$u_1(y)=D_{15} e^{\alpha_{11} y} + D_{16} e^{\alpha_{12} y} + D_{17} + D_{18} e^{\alpha_7 y} + D_{19} e^{\alpha_8 y} + D_{20} e^{\alpha_9 y} + D_{21} e^{\alpha_{10} y}$ (24)

$T_0(y)=D_1 e^{\alpha_1 y} + D_2 e^{\alpha_2 y}$ (25)

$C_0(y)=D_3 e^{\alpha_3 y} + D_4 e^{\alpha_4 y}$ (26)

$T_1(y)=D_{11}e^{\alpha_7 y} + D_{12}e^{\alpha_8 y}$ (27)

$C_1(y)=D_{13}e^{\alpha_9 y} + D_{14}e^{\alpha_{10} y}$ (28)

Invoking equations (21)-(26) into equations (11)-(13), we obtain the final solutions for the momentum, energy and specie equations as follows;

$u(y,t)= D_5e^{\alpha_5 y} + D_6e^{\alpha_6 y} + D_7e^{\alpha_1 y} + D_8e^{\alpha_2 y}+\epsilon\ (D_{15}e^{\alpha_{11} y} + D_{16}e^{\alpha_{12} y} + D_{17} + D_{18}e^{\alpha_7 y} + D_{19}e^{\alpha_8 y})e^{i\omega t}$ (29)

$T(y,t)= D_1e^{\alpha_1 y} + D_2e^{\alpha_2 y}+\epsilon\ (D_{11}e^{\alpha_7 y} + D_{12}e^{\alpha_8 y})\ e^{i\omega t}$ (30)

$C(y,t)= D_3e^{\alpha_3 y} + D_4e^{\alpha_4 y}+\epsilon(D_{13}e^{\alpha_9 y} + D_{14}e^{\alpha_{10} y})\ e^{i\omega t}$ (31)

The constants in the final solutions are clearly stated in the appendix

It is also very crucial to determine the physical effects at the walls of the channel. Hence, we obtain the physical effects by determining the skin friction coefficient and local Nusselt number as follows:

$C_f = \frac{\rho d^2 \tau_w}{\mu^2} = \left(\frac{du}{dy}\right)_{y=0,1}$, $Nu = \frac{d q_w}{k_f(T_w - T_0)} = -\left(\frac{dT}{dy}\right)_{y=0,1}$, $Sh = \frac{d q_w}{k_f(C_w - C_0)} = -\left(\frac{dC}{dy}\right)_{y=0,1}$, where $\tau_w = \mu\left(\frac{du}{dy}\right)_{y=0,d}$, $q_w = -k_f\left(\frac{dT}{dy}\right)_{y=0,d}$

III. RESULTS AND DISCUSSION

Figure 1 shows the effect of Peclet number variation on the temperature and concentration. The increase in the Peclet number shows a significant increase in the temperature and concentration. Figure 2 displays the effect of radiation parameter on the temperature. Increasing the radiation parameter decreases the temperature of the fluid. This is because high radiation of fluid temperature consequently reduces the temperature when it is radiating heat at higher level. Figure 3 depicts the heat generation parameter increase the temperature profile on the increase of heat generation. Figure 4 shows the effective thermal conductivity. Increasing the thermal conductivity increases the fluid temperature. Figure5 depicts the volume fraction of copper nanoparticles. Increase in the volume fraction nanoparticles did not consequently change the temperature of the fluid. Figures 6, 7, 8, 9, 10 show the Peclet number owing to the concentration of the fluid, chemical reaction parameter, Schmidt number, frequency of oscillation and volume fraction of copper respectively, it is seen that incrementally varying the Peclet number, chemical reaction, Schmidt number, frequency of oscillation and volume fraction of copper consequently increase the fluid concentration. Figure 11 presents the increase in the Peclet number increases the velocity of the fluid. The radiation parameter decreases the velocity of the fluid as shown in figure 12 due to a decrease in the momentum boundary layer. Variation in the heat generation and effective thermal conductivity parameters as shown in the figures 13 and 14. Varying the heat generation parameter and effective thermal conductivity did not significantly cause any change in the velocity. Increasing the Reynolds number decreases the velocity of the fluid as shown in figure 15. Figures 16 and 17 show the effect of the chemical reaction parameter and Schmidt number on the velocity profile. It is seen clearly that increasing the chemical reaction parameter and Schmidt number consequently decrease the velocity profile. The presence of Lorentz force in the magnetic field deters the motion of the fluid owing to the friction created by the Lorentz force as displays in figure 18. Increasing the Grashof number increases the velocity of the fluid owing the increase in the thermal buoyancy which in turns increases the boundary layer, hence leading to the increase in the velocity of the fluid as seen in figures 19 and 20. The volume fraction of copper nanofluid particles is shown in figure 22. Increasing the volume fraction decreases the fluid velocity. Figure 21 shows no change in the velocity for consequent variation in the porosity on the velocity. Figure 23 shows the impact of the frequency of oscillation on the velocity. Increasing the frequency of oscillation decreases the fluid velocity. The figure 24 shows the different shapes of copper. It is seen that increasing the different shapes of copper increases the velocity of the fluid.

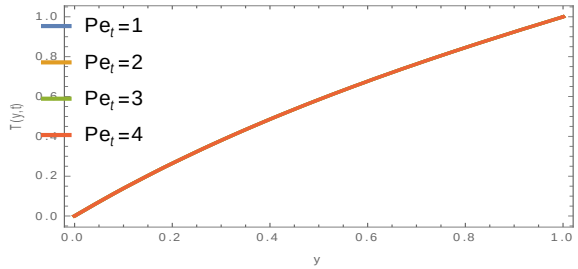

Figure1: Dependence of temperature on coordinate with Peclet number in water based nanofluid when N=1.07, S=0.62, λn=1,t=0.1,$\epsilon = 0.5$

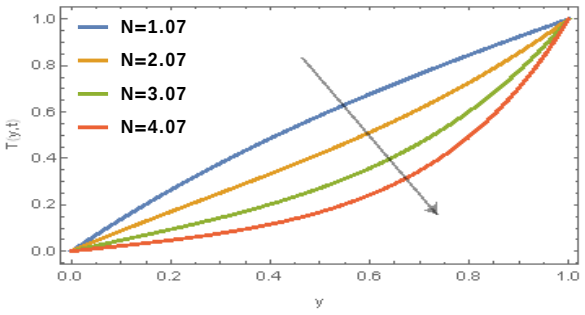

Figure2: Dependence of temperature on coordinate with thermal radiation(N) in water based nanofluid when Pe=1, S=0.62, λn=1,t=0.1,$\epsilon = 0.5$

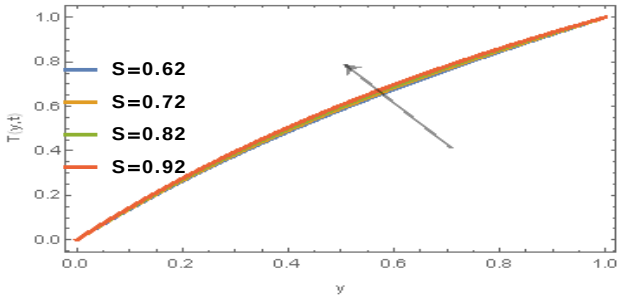

Figure3: Dependence of temperature on coordinate with heat generation parameter in water based nanofluid when N=1.07, Pe=1, λn=1,t=0.1,$\epsilon = 0.5$

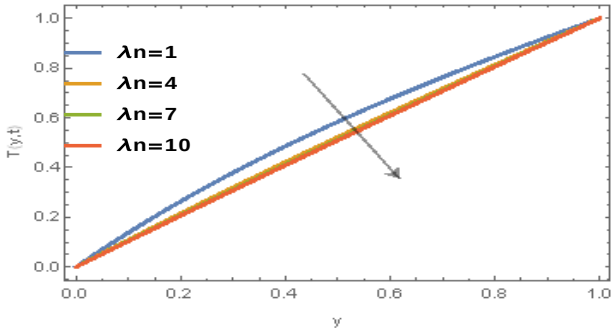

Figure4: Dependence of temperature on coordinate with effective thermal conductivity in water based nanofluid when N=1.07, S=0.62, Pe=1,t=0.1,$\epsilon = 0.5$

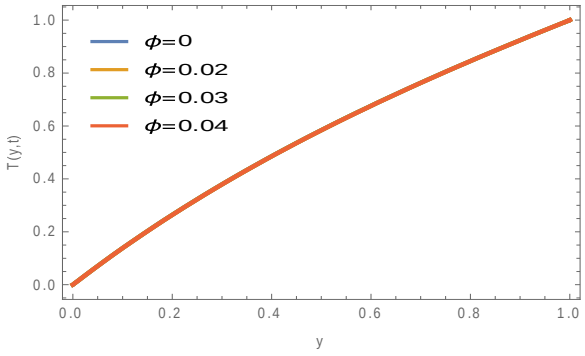

Figure5: Dependence of temperature on coordinate with ϕ of Cu in water based nanofluid when N=1.07, S=0.62, λn=1,t=0.1,$\epsilon = 0.5$

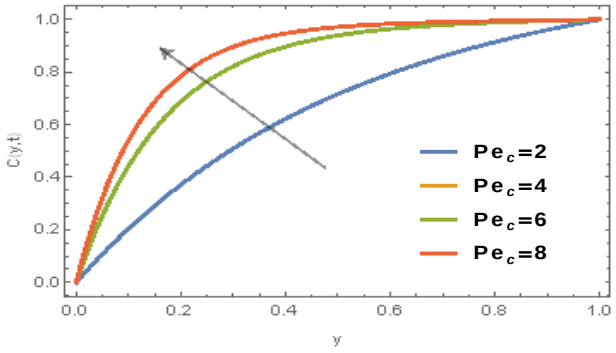

Figure6: Dependence of concentration on coordinate with Pe_c in water based nanofluid when Kr=1.21, Sc=0.15, ω=0.2, t=0.1,$\emptyset = 0,\epsilon = 0.5$

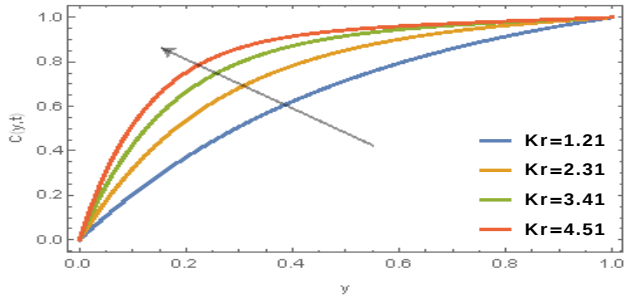

Figure7: Dependence of concentration on coordinate with Kr in water based nanofluid when Pe_c=2, Sc=0.15, ω=0.2, t=0.1,$\emptyset = 0,\epsilon = 0.5$

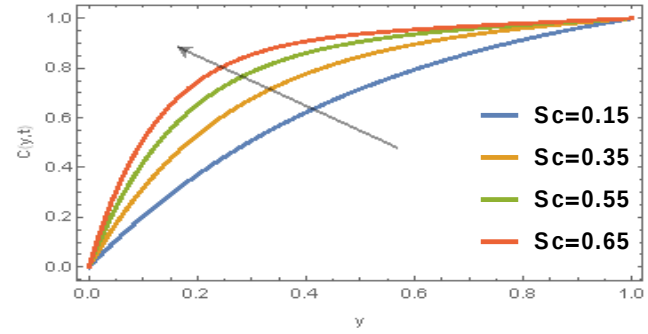

Figure8: Dependence of concentration on coordinate with Sc in water based nanofluid when Pe_c=2, Kr=1.21, ω=0.2, t=0.1,$\emptyset = 0,\epsilon = 0.5$

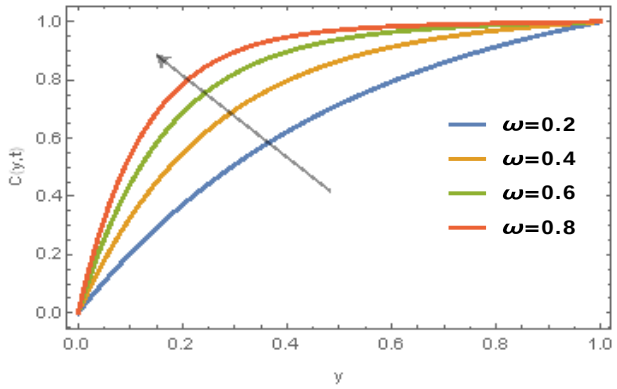

Figure9: Dependence of concentration on coordinate with ω in water based nanofluid when Pe_c=2, Sc=0.15, Kr=1.21, ω=0.2, t=0.1,$\emptyset = 0,\epsilon = 0.5$

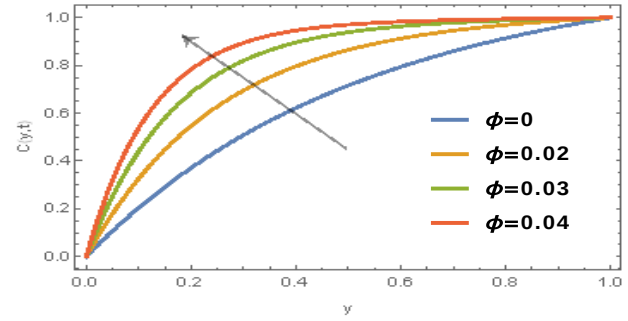

Figure10: Dependence of concentration on coordinate with Ø of Cu in water based nanofluid when Pe_c=2, Sc=0.15, Kr=1.21, ω=0.2, t=0.1,$\emptyset = 0,\epsilon = 0.5$

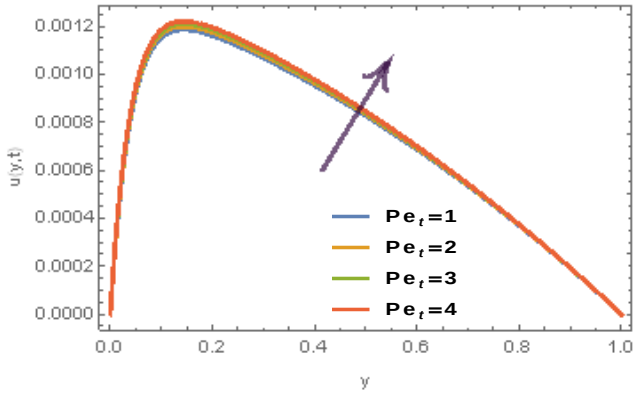

Figure11: Dependence of velocity on coordinate with Peclet number in water based nanofluid when N=1.07, S=0.62, λn=1,t=0.1,ϵ = 0.5,Gr=0.03,M=10,K=1.49,Re=100, ω = 0.2,, Pe$_c$ = 2, Gm=0.05,Sc=0.15, $\emptyset$ = 0, Kr=1.21

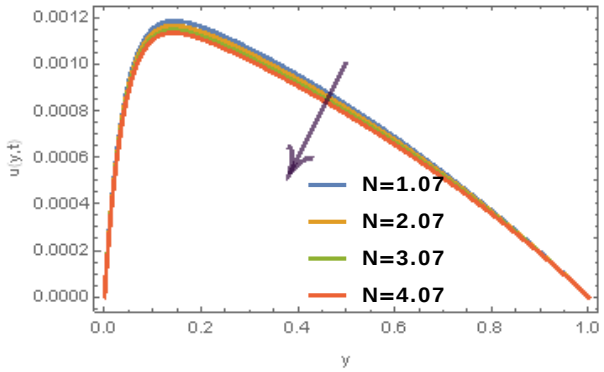

Figure12: Dependence of velocity on coordinate with N in water based nanofluid when S=0.62, λn=1,t=0.1,ϵ = 0.5,Gr=0.03,M=10,K=1.49,Re=100, ω = 0.2, Pe_t = 1, Pe_c = 2, Gm=0.05,Sc=0.15, $\emptyset$ = 0, Kr=1.21

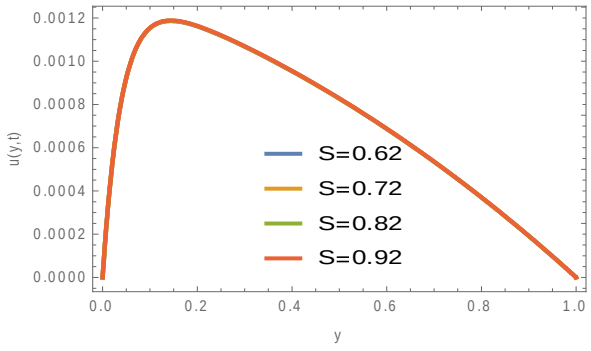

Figure13: Dependence of velocity on coordinate with S in water based nanofluid when N=1.07,, λn=1,t=0.1,ϵ = 0.5,Gr=0.03,M=10,K=1.49,Re=100, ω = 0.2, Pe_t = 1, Pe_c = 2, Gm=0.05,Sc=0.15, $\emptyset$ = 0, Kr=1.21

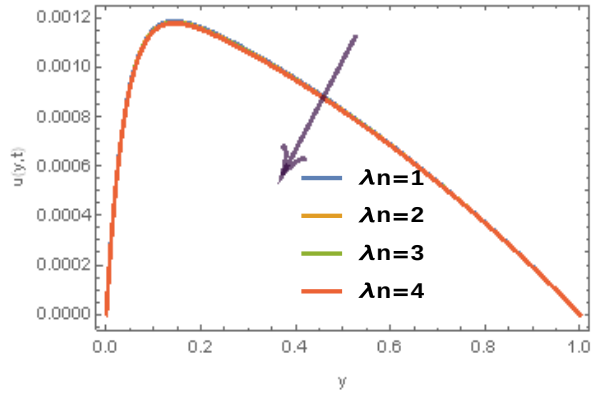

Figure14: Dependence of velocity on coordinate with effective thermal conductivity in water based nanofluid when N=1.07, S=0.62,t=0.1,ϵ = 0.5,Gr=0.03,M=10,K=1.49,Re=100, ω = 0.2, Pe_t = 1, Pe_c = 2, Gm=0.05,Sc=0.15, $\emptyset$ = 0, Kr=1.21

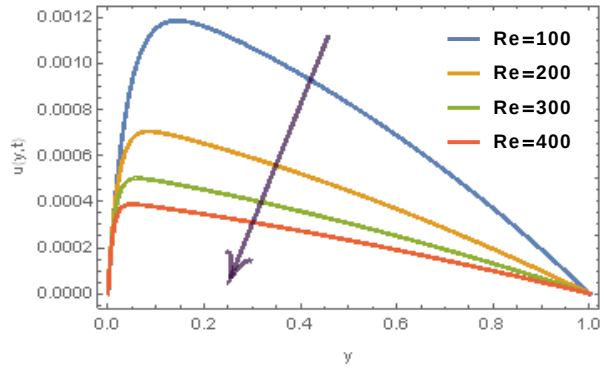

Figure15: Dependence of velocity on coordinate with Reynolds number in water based nanofluid when N=1.07, S=0.62, λn=1,t=0.1,ϵ = 0.5,Gr=0.03,M=10,K=1.49, ω = 0.2, Pe_t = 1, Pe_c = 2, Gm=0.05,Sc=0.15, $\emptyset$ = 0, Kr=1.21

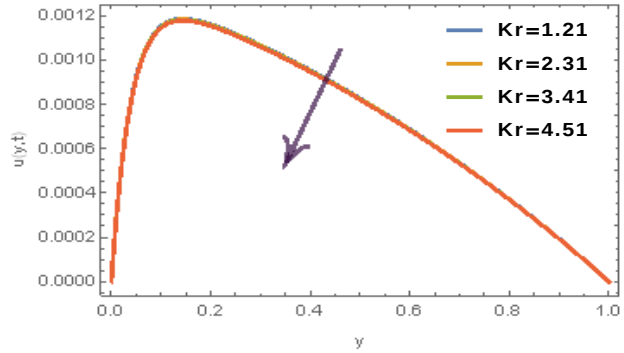

Figure16: Dependence of velocity on coordinate with Chemical reaction parameter in water based nanofluid when N=1.07, S=0.62, λn=1,t=0.1,ϵ = 0.5,Gr=0.03,M=10,K=1.49,Re=100, ω = 0.2, Pe_t = 1, Pe_c = 2, Gm=0.05,Sc=0.15, $\emptyset$ = 0

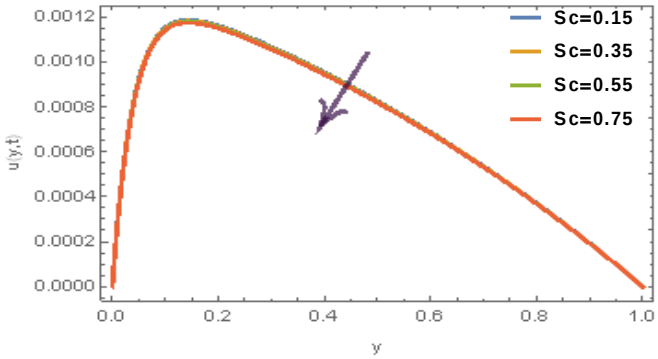

Figure17: Dependence of velocity on coordinate with Schmidt number in water based nanofluid when N=1.07, S=0.62, λn=1,t=0.1,ϵ = 0.5,Gr=0.03,M=10,K=1.49,Re=100, $\omega = 0.2$, $Pe_t = 1$, $Pe_c = 2$, Gm=0.05, $\emptyset = 0$, Kr=1.21

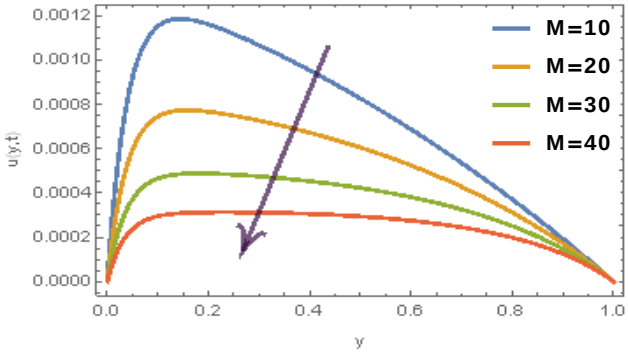

Figure18: Dependence of velocity on coordinate with M in water based nanofluid when N=1.07, S=0.62, λn=1,t=0.1,ϵ = 0.5,Gr=0.03,M=10,K=1.49,Re=100, $\omega = 0.2$, $Pe_t = 1$, $Pe_c = 2$, Gm=0.05,Sc=0.15, $\emptyset = 0$, Kr=1.21

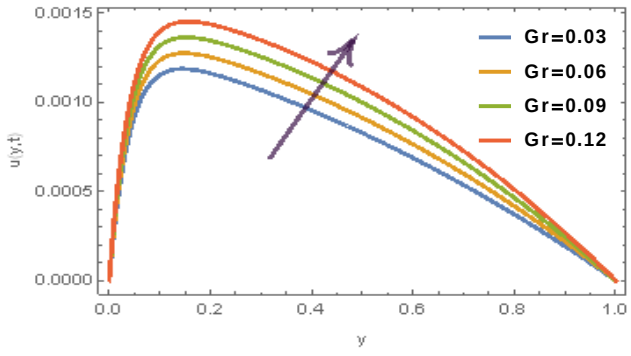

Figure19: Dependence of velocity on coordinate with Gr in water based nanofluid when N=1.07, S=0.62, λn=1,t=0.1,ϵ = 0.5, M=10,K=1.49,Re=100, $\omega = 0.2$, $Pe_t = 1$, $Pe_c = 2$, Gm=0.05,Sc=0.15, $\emptyset = 0$, Kr=1.21

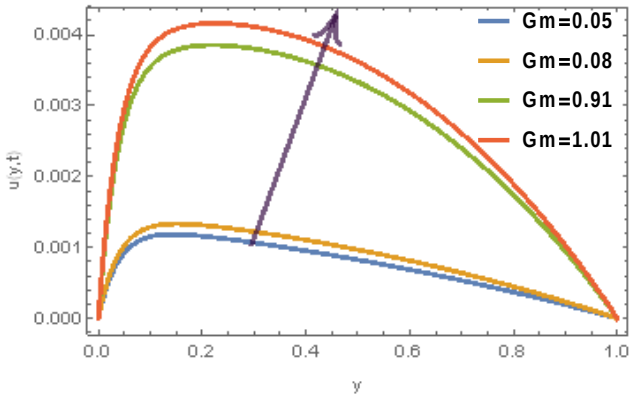

Figure20: Dependence of velocity on coordinate with Gm in water based nanofluid when N=1.07, S=0.62, λn=1,t=0.1,ϵ = 0.5,Gr=0.03,M=10,K=1.49,Re=100, $\omega = 0.2$, $Pe_t = 1$, Pe_c = 2,Sc=0.15, $\emptyset = 0$, Kr=1.21

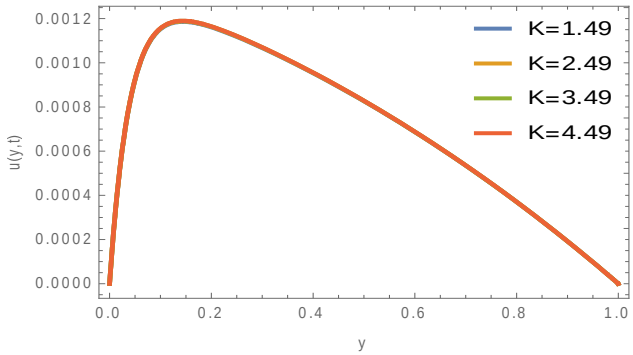

Figure21: Dependence of velocity on coordinate with K in water based nanofluid when N=1.07, S=0.62, λn=1,t=0.1,ϵ = 0.5,Gr=0.03,M=10 ,Re=100, $\omega = 0.2$, $Pe_t = 1$, $Pe_c = 2$, Gm=0.05,Sc=0.15, $\emptyset = 0$, Kr=1.21

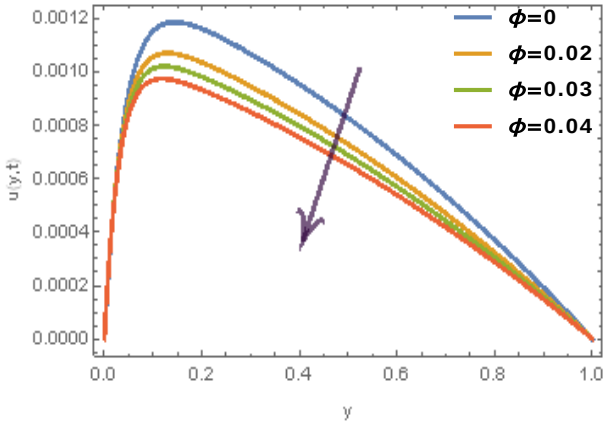

Figure22: Dependence of velocity on coordinate with $\emptyset$ of Cu in water based nanofluid when N=1.07, S=0.62, λn=1,t=0.1,ϵ = 0.5,Gr=0.03,M=10,K=1.49,Re=100, $\omega = 0.2$, $Pe_t = 1$, $Pe_c = 2$, Gm=0.05,Sc=0.15 , Kr=1.21

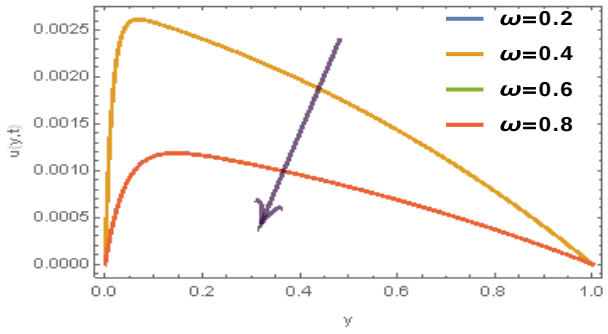

Figure23: Dependence of velocity on coordinate with ω in water based nanofluid when N=1.07, S=0.62, λn=1,t=0.1,ϵ = 0.5,Gr=0.03,M=10,K=1.49,Re=100, $Pe_t = 1$, $Pe_c = 2$, Gm=0.05,Sc=0.15 , Kr=1.21, $\emptyset = 0$

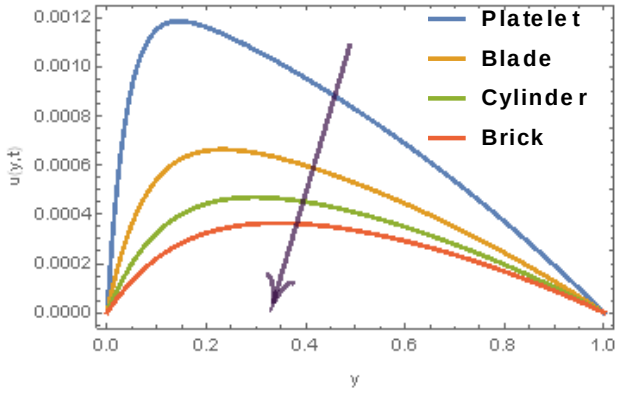

Figure24: Dependence of velocity on coordinate with shape factors in water based nanofluid when N=1.07, S=0.62, λn=1,t=0.1,ϵ = 0.5,Gr=0.03,M=10,K=1.49,Re=100, $Pe_t = 1$, $Pe_c = 2$, Gm=0.05,Sc=0.15 , Kr=1.21, $\emptyset = 0$

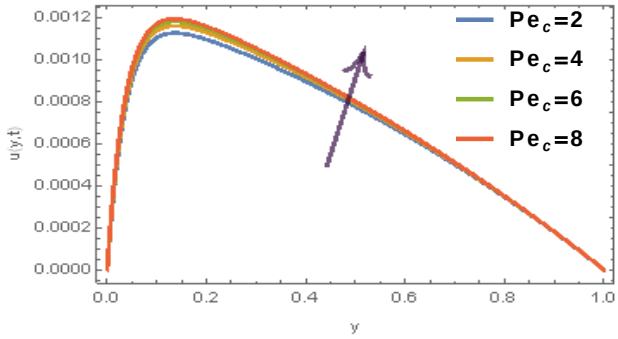

Figure25: Dependence of velocity on coordinate withPe_c in water based nanofluid when N=1.07, S=0.62, λn=1,t=0.1,ϵ = 0.5,Gr=0.03,M=10,K=1.49,Re=100, $Pe_t = 1$, Gm=0.05,Sc=0.15 , Kr=1.21, $\emptyset = 0$

IV. CONCLUSION

In this paper, we have successfully analyzed the entropy generation on thermal transfer in MHD natural convection of Cu-H_2O nanofluid in a porous channel with heat generation/absorption. The governing equations were analytically solved and expressed in exponential and complimentary functions. From the foregoing, it is observed that:

1. Thermal radiation decreased the temperature of the fluid.
2. Heat generation/absorption parameter increased the temperature of the fluid.
3. The effective thermal conductivity increased the temperature of the fluid.
4. Peclet number decreased the velocity of the fluid.
5. Reynolds number decreased the fluid velocity.
6. Peclet number, Reynolds number and heat generation rapidly increased and decreased the entropy generation at the lower and upper plates respectively.
7. Increasing the volume fraction of copper leads to an increase in the concentration of the fluid.

REFERENCES

[1] Aaiza, G.; Khan, I & Shafie, S.(2015). Energy transfer in mixed convection MHD flow of nanofluid containing different shapes of nanoparticles in a channel filled with saturated porous medium. Nanoscale research letters,2(2015), 1-16.

[2] Achogo, W. H.; Adikabu, I. N.; Awortu, I. & Eleonu, B. C.(2020). Soret effect on MHD free convection through a porous inclined channel in the presence of thermal radiation. International journal of research and innovation in applied, 5(7),117-124.

[3] Buggaramulu J. & Venkata M. K.(2017). MHD convection flow of Kuvshinski fluid past an infinite vertical porous plate with radiation and chemical reaction effects. International journal on recent and innovation trends in computing and communication, 5(9),64-74.

[4] Choi SUS (1995). Enhancing thermal conductivity of fluids with nanoparticle, in: D.A. Siginer, H.P. Wang (Eds.), Developments and Applications of Non- Newtonian Flows. ASME FED, 66(1995),99–105.

[5] Constantin F.; Dumitru V. & Waqas A. A.(2017). Natural convection flow of fractional nanofluids over an isothermal vertical plate with thermal radiation. Applied Sciences,7(247),1-13. DOI:10.3390/app7030247

[6] Kathyayani, G. & Praveen B.D.M.(2016). Heat and mass transfer on mhd flow over an infinite rotating oscillating vertical porous plate. International journal of advanced research, 4(6),1078-1086. DOI:10.21474/IJAR01

[7] Khan, S. M.; Karim, I; Ali, E. L. & Islam, A.(2012). Unsteady MHD free convection boundary – layer flow of a nanofluid along a stretching sheet with thermal radiation and viscous dissipation effects. International nano letters, 2(2012), 1-9.

[8] Latiff, N. A.; Uddin, M. J. & Ismail, A. I.(2016). Stefan blowing effect on bioconvective flow of nanofluid over a solid rotating stretchable disk. Propulsion and power research, 5(4), 267-278.

[9] Madhura, K. R.; Babitha. A. & Iyenga, S. S.(2017). Impact of heat and mass transfer on mixed convective flow of nanofluid through porous medium. International Journal of Applied Computational Mathematics, 10(2), 10-11. DOI:10.1007/s40819-017-0424-3

[10] Madhura, K. R.; Kalpana, G. & Soniya, H.(2020). Heat and mass transfer of MHD fluid flow under the influence of radiative effect and different pressure gradients. Studies in Indian Place Names,40(10),427-439.

[11] Malvandi, A.; Ganji, D. D.; Hedayati, F & Rad, Y. E.(2013). An analytical study on entropy generation of nanofluids over a flat plate. Alexandria engineering journal, 52(2013), 595-604.

[12] Murugesan, T. & Kumar, D. M.(2019). Viscous dissipation and joule heating effects on MHD flow of a thermo-solutal stratified nanofluid over an exponentially stretching sheet with radiation and heat generation/absorption. World schientific news, 129(2019),193-210.

[13] Naik, M. T. & Sundar, L. S. (2011). Investigation into thermophysical properties of glycol based CuO nanofluid for heat transfer applications. World AcadScience Engineer Technology, 59(2011),,440–446.

[14] Reddy M. G. & Reddy N. B.(2011). Mass transfer and heat generation effects on MHD free convection flow past an inclined vertical surface in a porous medium. Journal of applied fluid mechanics, 4(2), 7-11.

[15] Sharma R. & Isahk, A.(2014). Second order slip flow of Cu-Water nanofluid over a stretching sheet with heat transfer. WSEAS transactions on fluid mechanics, 9(2014), 26-33.

[16] Shateyi, S.; Motsa, S. S. & Makukula, Z.(2015). On spectral relaxation method for entropy generation on MHD flow and heat transfer of a Maxwell fluid. Journal of applied fluid mechanics, 8(1), 21-31.

[17] Srinivasacharya, D. & Bindu H. K.(2015). Entropy generation in a micropolar fluid flow through an inclined channel. Alexandria engineering journal, 55(2016), 973-982.

[18] Vajjha, R.S. & Das, D.K .(2009). Experimental determination of thermal conductivity of three nanofluids and development of new correlations. International journal of heat and mass transfer,, 52(2009), 4675-4682.

APPENDIX

$$\alpha_1 = \frac{\frac{-m_2 m_1 Pe}{\lambda n} + \sqrt{\left(\frac{m_2 m_1 Pe}{\lambda n}\right)^2 - 4\left(\frac{N^2 - S}{\lambda n}\right)}}{2}, \qquad \alpha_7 = \frac{\frac{-m_2 m_1 Pe}{\lambda n} + \sqrt{\left(\frac{m_2 m_1 Pe}{\lambda n}\right)^2 - 4\left(\frac{m_1 Pei\omega - N^2 + S}{\lambda n}\right)}}{2},$$

$$\alpha_2 = \frac{\frac{-m_2 m_1 Pe}{\lambda n} - \sqrt{\left(\frac{m_2 m_1 Pe}{\lambda n}\right)^2 - 4\left(\frac{N^2 - S}{\lambda n}\right)}}{2}, D_{11} = D_{12} = 0, \alpha_{11} = \frac{-m_2 m_4 Re + \sqrt{(m_2 m_4 Re)^2 - 4\left(M^2 + \frac{m_5}{K} + m_4 Rei\omega\right)}}{2m_5},$$

$$\alpha_8 = \frac{\frac{-m_2 m_1 Pe}{\lambda n} - \sqrt{\left(\frac{m_2 m_1 Pe}{\lambda n}\right)^2 - 4\left(\frac{m_1 Pei\omega - N^2 + S}{\lambda n}\right)}}{2}, \alpha_{12} = \frac{-m_2 m_4 Re - \sqrt{(m_2 m_4 Re)^2 - 4\left(M^2 + \frac{m_5}{K} + m_4 Rei\omega\right)}}{2m_5}$$

$$D_2 = \frac{1}{e^{\alpha_2} - e^{\alpha_1}}, D_{18} = \frac{-m_6 Gr D_{11}}{m_5 {\alpha_7}^2 + -m_2 m_4 Re\alpha_7 - \left(M^2 + \frac{m_5}{K} + m_4 Rei\omega\right)}, D_{19} = \frac{-m_6 Gr D_{11}}{m_5 {\alpha_8}^2 + -m_2 m_4 Re\alpha_8 - \left(M^2 + \frac{m_5}{K} + m_4 Rei\omega\right)} \qquad D_{17} = \frac{\lambda}{\left(M^2 + \frac{m_5}{K} + m_4 Rei\omega\right)},$$

$$D_1 = \frac{-1}{e^{\alpha_2} - e^{\alpha_1}}, \alpha_5 = \frac{-m_2 m_4 Re + \sqrt{(m_2 m_4 Re)^2 - 4m_5\left(M^2 + \frac{m_5}{K}\right)}}{2m_5}, \alpha_6 = \frac{-m_2 m_4 Re - \sqrt{(m_2 m_1 Re)^2 - 4m_5\left(M^2 + \frac{m_5}{K}\right)}}{2m_5},$$

$$D_7 = \frac{m_6 Gr A_1}{m_5 {\alpha_1}^2 + -m_2 m_4 Re\alpha_1 - \left(M^2 + \frac{m_5}{K}\right)}, D_8 = \frac{-m_6 Gr A_1}{m_5 {\alpha_2}^2 + -m_2 m_4 Re\alpha_2 - \left(M^2 + \frac{m_5}{K}\right)},$$

$$D_6 = \frac{1}{e^{\alpha_6} - e^{\alpha_5}}[D_7 e^{\alpha_5 y} + D_8 e^{\alpha_5 y} - D_7 e^{\alpha_1 y} - D_8 e^{\alpha_2 y}], \qquad D_5 = \frac{1}{e^{\alpha_6} - e^{\alpha_5}}[D_7 e^{\alpha_5 y} + D_8 e^{\alpha_5 y} - D_7 e^{\alpha_1 y} - D_8 e^{\alpha_2 y}] - [D_7 + D_8],$$